

# Creation and annealing of metastable defect states in $\text{CH}_3\text{NH}_3\text{PbI}_3$ at low temperatures

F. Lang, O. Shargaieva, V.V. Brus, J. Rappich, N.H. Nickel

Helmholtz-Zentrum Berlin für Materialien und Energie GmbH

Institut für Silizium-Photovoltaik

Kekuléstr. 5, 12489 Berlin, Germany

## Abstract

Methylammonium lead iodide ( $\text{CH}_3\text{NH}_3\text{PbI}_3$ ), an organic-inorganic perovskite widely used for optoelectronic applications, is known to dissociate under illumination with light at photon energies around 2.7 eV and higher. Here, we show that photo-induced dissociation is not limited to ambient temperatures but can be observed even at 5 K. The photo-induced dissociation of N – H bonds results in the formation of metastable states. Photoluminescence (PL) measurements reveal the formation of defect states that are located 100 meV within the band gap. This is accompanied by a quenching of the band-to-band PL by one order of magnitude. Defect generation is reversible and annealing at 30 K recovers the band-to-band PL, while the light-induced defect states disappear concurrently.

*Keywords:  $\text{CH}_3\text{NH}_3\text{PbI}_3$ , organic-inorganic perovskite, photo-induced degradation, defects, defect annealing*

Organic-inorganic perovskites, such as methylammonium lead iodide ( $\text{CH}_3\text{NH}_3\text{PbI}_3$ ), have attracted great interest within the last years. With a direct band gap, a large absorption coefficient,<sup>1</sup> and long diffusion lengths,<sup>2-4</sup> this material is particularly well suited for solar cells. Power conversion efficiencies have jumped beyond 22.1 % recently.<sup>5</sup> However, a variety of stimuli cause degradation of organic-inorganic perovskites.<sup>6</sup> Recently, instability mechanisms at elevated temperatures, in moisture, in oxygen, and under high energy irradiation have been re-visited.<sup>6</sup> Interestingly, even in the absence of oxygen and moisture, illumination deteriorates  $\text{CH}_3\text{NH}_3\text{PbI}_3$ . Gas-effusion and Fourier-transformed infrared (FT-IR) measurements have unambiguously shown that illumination with a photon energy of  $E_{\text{ph}} \geq 2.72$  eV results in the dissociation of methylammonium ions into  $\text{CH}_3\text{NH}_2$  and hydrogen.<sup>7</sup> At room temperature (RT), both fragments are highly mobile and diffuse out of the samples.<sup>7</sup>

Commonly, light-induced degradation mechanisms exhibit activated behavior and one would expect that degradation would cease at low temperatures. Therefore, we investigated the effect of illumination on  $\text{CH}_3\text{NH}_3\text{PbI}_3$  at low temperatures ( $T = 5$  K). Interestingly, our data clearly show that illumination with photon energies of  $E_{\text{ph}} \geq 2.7$  eV causes the generation of localized defects at  $T = 5$  K that most likely is due to the dissociation of  $\text{CH}_3\text{NH}_3^+$  ions and the formation of I – H complexes. According to photoluminescence (PL) spectra, the localized defects reside about 100 meV within the band gap. Upon annealing at  $T = 30$  K the localized defects disappear, which is accompanied by a recovery of the band-to-band PL. This suggests that photo-induced degradation of  $\text{CH}_3\text{NH}_3\text{PbI}_3$  is reversible at low temperatures and the introduced defect states are metastable.

Polycrystalline  $\text{CH}_3\text{NH}_3\text{PbI}_3$  layers were prepared on cleaned single crystal silicon substrates. An equimolar solution of  $\text{PbI}_2$  and  $\text{CH}_3\text{NH}_3\text{I}$  was used for the spin-coating following the anti-solvent procedure pioneered by Jeon et al.<sup>8</sup> Details on the preparation and the performance of solar cells are described elsewhere.<sup>4,9</sup> The perovskite layers had a thickness of about 300 nm and the average grain size amounted to about 250 nm. To avoid degradation, the specimens were prepared and mounted on a cryostat from Oxford instruments inside a glove-box at an  $\text{O}_2$  and  $\text{H}_2\text{O}$  content well below 0.1 ppm. Without exposure to air, the specimens were cooled down to 5 K. Unless otherwise noted, PL spectra were recorded at 5 K using a pulsed dye

laser with a wavelength of  $\lambda_{\text{exc}} = 500$  nm and a repetition rate of 11 Hz. Light-induced degradation was performed with an LED with a photon energy of  $E_{\text{ph}} = 3.4$  eV. To gain information on nitrogen-hydrogen bonding some specimens were characterized with Fourier-transform infrared (FT-IR) measurements.

Photoluminescence spectra of as-prepared specimens reveal an intense PL signal ( $I_{\text{PL}}$ ) at  $E_{\text{ph}} = 1.61$  eV due to the direct band-to-band transition in the orthorhombic phase of  $\text{CH}_3\text{NH}_3\text{PbI}_3$  (solid curve in Fig. 1).<sup>10</sup> The dashed red line in Fig. 1 depicts a PL spectrum after degradation with light from an LED with a photon energy of  $E_{\text{ph}} = 3.4$  eV. The entire specimen was illuminated for 30 min, which resulted in the generation of a second PL peak centered at  $E_{\text{ph}} = 1.51$  eV with a full width at half maximum (FWHM) of 19 meV. In addition, the band-to-band related PL is quenched by almost one order of magnitude.

Surprisingly, the light-induced degradation is reversible. A short anneal at  $T = 30$  K for 5 min causes the band-to-band PL to recover almost to its initial value, while the defect-related PL at  $E_{\text{ph}} = 1.51$  eV disappears completely (dotted curve in Fig. 1).

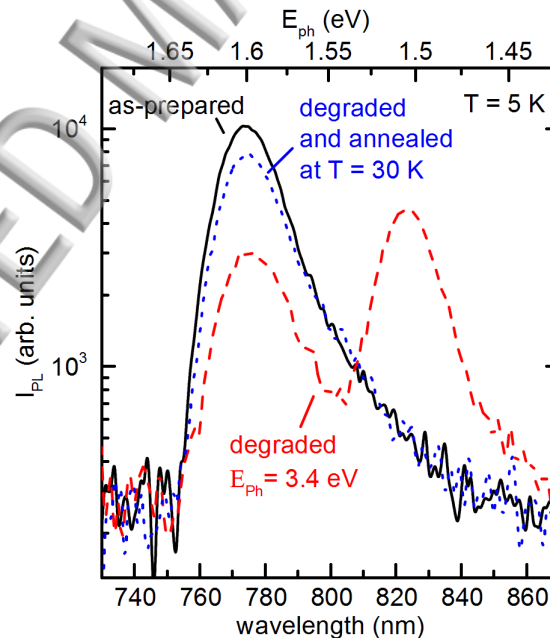


Figure 1: Photoluminescence spectra of as-prepared (black solid line), degraded (red dashed line), and annealed  $\text{CH}_3\text{NH}_3\text{PbI}_3$  thin films (blue dotted line). A pulsed dye laser with a wavelength of  $\lambda_{\text{exc}} = 500$  nm and a laser fluence of  $2.6$  mJ/cm<sup>2</sup> was used for the excitation. Light-induced degradation was performed with an LED at  $E_{\text{ph}} = 3.4$  eV for 30 min. Annealing was done by heating the sample to  $T = 30$  K for 5 min. All PL spectra were measured at  $T = 5$  K.

It is conceivable that the PL at 1.51 eV originates from photo-induced defects located 100 meV within the band gap. To corroborate this interpretation, PL spectra were recorded as a function of the excitation energy. Fig. 2 depicts PL spectra for different excitation fluences. All spectra were recorded after light-induced degradation for 30 min. The red and green shaded areas represent least-square fits of the data to Voigt profiles. At the lowest excitation fluence of  $f = 2.6 \text{ mJ/cm}^2$ , the PL at 1.51 eV exceeds the intensity of the band-to-band related transition at 1.61 eV. For higher excitation energies both PL features increase in intensity. However, already for an excitation laser-fluence of  $f = 15.3 \text{ mJ/cm}^2$  the ratio of the two PL bands changes and the band-to-band recombination process dominates the spectrum (Fig. 2). For higher laser fluences ( $f \geq 22.6 \text{ mJ/cm}^2$ ) the intensity at 1.51 eV is almost negligible compared to the band-to-band PL located at 1.61 eV.

In case of radiative recombination, the radiation rate defined as  $R = \frac{dn}{dt}$  is given by  $R_{\text{rad}} \propto np \propto f^2$ , where  $n$  and  $p$  denote the density of photo-generated electrons and holes, respectively, and  $f$  is the excitation fluence.<sup>11,12</sup> On the other hand, if recombination is dominated by localized states in the band gap the radiation rate is given by  $R_{\text{defect}} \propto Nn \propto f$ . Here  $N$  represents the density of localized states and  $n = p$  is the concentration of photo-generated charged carriers.<sup>11,12</sup>

To elucidate the nature of the PL the ratio of the integrated PL peaks centered at 1.61 and 1.51 eV,  $A^{1.61}/A^{1.51}$ , is plotted as a function of  $f$  in the inset of Fig. 2. In the double logarithmic plot, the data can be fitted by a straight line with a slope of  $S \approx 1.1 \pm 0.3 \text{ cm}^2 / \text{mJ}$ . This dependence requires a radiative and a defect-related luminescence process according to  $A_{\text{rad}}/A_{\text{defect}} \propto f^2 / f$ . Hence, it indicates that the PL centered at 1.51 eV originates from a photo-induced defect located about 100 meV within the band gap of the perovskite.

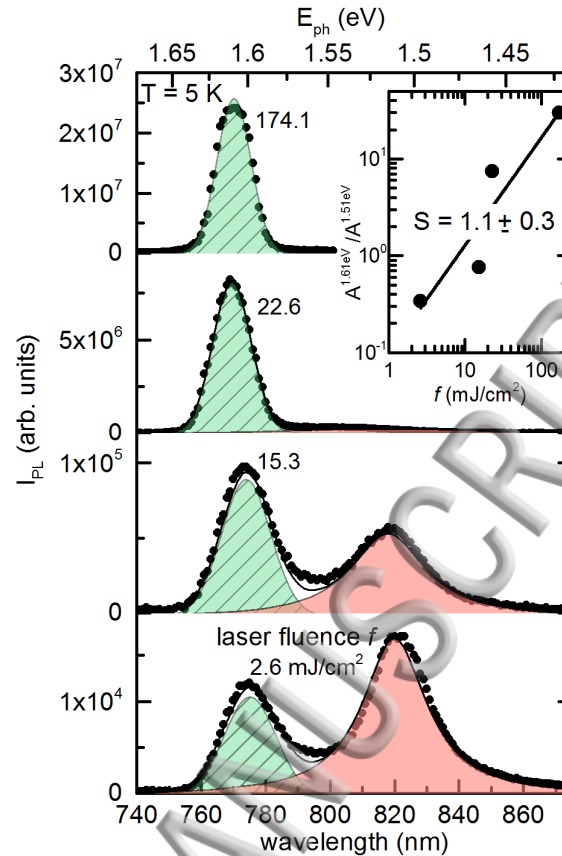


Figure 2: Photoluminescence spectra of a degraded  $\text{CH}_3\text{NH}_3\text{PbI}_3$  specimen. The excitation fluence was varied from 2.6, 15.3, 22.6, to 174.1  $\text{mJ}/\text{cm}^2$ . The inset depicts the ratio  $A^{1.6}/A^{1.51}$  of the integrated PL peaks at 1.6 and 1.51 eV as a function of the laser fluence,  $f$ . Degradation was performed with a nitrogen laser at  $E_{\text{ph}} = 3.7$  eV and a fluence of  $\approx 9$   $\text{mJ}/\text{cm}^2$  for 30 min. The data were measured at  $T = 5$  K.

Although the data presented in Fig. 1 shows that light-induced defect generation of  $\text{CH}_3\text{NH}_3\text{PbI}_3$  is reversible, the anneal at  $T = 30$  K does not completely restore the initial state. The band-to-band PL does not fully recover and its intensity is about 24 % smaller after light-induced degradation and subsequent annealing. To elucidate the underlying mechanism FT-IR measurements were performed prior to and after light-induced degradation. FT-IR spectra taken prior to (black solid curve) and after prolonged illumination (red dashed curve) are shown in Fig. 3(a). For clarity, the spectrum of the degraded sample was shifted vertically. The spectra show the N – H stretching vibrational modes of the  $\text{CH}_3\text{NH}_3^+$  ions. To visualize the changes due to degradation, the spectrum of the degraded sample was normalized to the one measured for the as-prepared specimen.

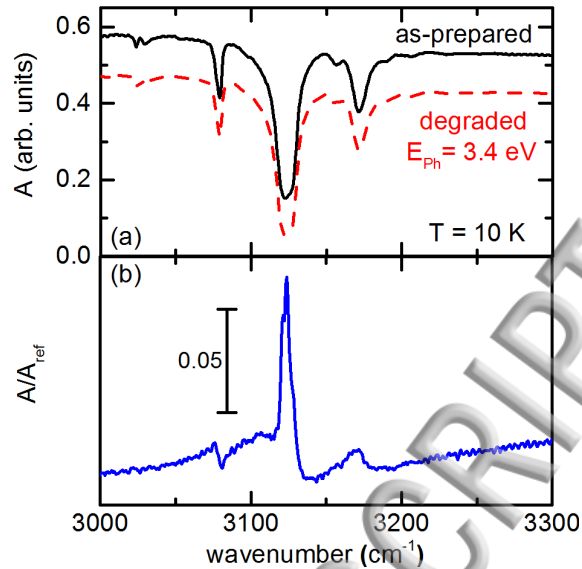


Fig. 3. FT-IR spectra in the range of the N-H vibrational modes of  $\text{CH}_3\text{NH}_3\text{PbI}_3$  taken before (black solid curve) and after light-induced degradation (red dashed curve) (a). Note that the spectrum obtained after degradation was shifted vertically for better visualization. For the degradation, an LED with a photon energy of 3.4 eV was used and the specimen was exposed for 10 min. (b) shows the relative IR absorption due to the degradation normalized to the data of the as-prepared sample. The measurements were taken at  $T = 10$  K.

The resulting relative change of the IR absorption,  $A/A_{\text{ref}}$ , is plotted in Fig. 3(b). Because of the used normalization, a signal gain of the N – H vibrational modes represents a loss of  $\text{NH}_3^+$  centers in the sample. This indicates that prolonged illumination causes the dissociation of  $\text{CH}_3\text{NH}_3^+$  ions. Interestingly, it is consistent with a recent report that showed the light-induced dissociation of  $\text{CH}_3\text{NH}_3^+$  ions at room temperature (RT).<sup>7</sup> According to our data, this dissociation mechanism is not limited to RT. Since the dissociation of  $\text{CH}_3\text{NH}_3^+$  ions also occurs at very low temperatures our data suggest that the light-induced dissociation of  $\text{CH}_3\text{NH}_3\text{PbI}_3$  is not limited by a thermal barrier.

The experimental results presented above show unambiguously that prolonged illumination at 5 K causes the formation of localized defects in the band gap of  $\text{CH}_3\text{NH}_3\text{PbI}_3$ . The light-induced defects are metastable and they disappear after a short anneal at 30 K. However, PL experiments show that the band-to-band related PL does not recover completely. According to FT-IR measurements, this is due to the dissociation of the organic cations. This is consistent with a recent report on light-induced degradation experiments performed at RT.<sup>7</sup>

Recently, it has been shown that the light-induced dissociation of  $\text{CH}_3\text{NH}_3^+$  ions is due to trapping of electrons in the N – H antibonding orbitals. At RT the resulting  $\text{CH}_3\text{NH}_2$  and hydrogen atoms migrate out of the specimen.<sup>7</sup> Since the experiments presented above were carried out at low temperatures ( $T \leq 30$  K) out-diffusion of organic molecules or hydrogen atoms can be ruled out. Also, because of the low temperatures the migration of iodine or lead vacancies can be excluded since the corresponding diffusion barriers are in the range of 0.1 to 0.8 eV.<sup>13</sup> Hence, the dissociation fragments of the organic cation, namely  $\text{CH}_3\text{NH}_2$  and H, remain in the perovskite lattice. Based on first principles calculations it has been suggested that  $\text{CH}_3\text{NH}_2$  is stable in the perovskite lattice and resides in a substitutional position at the  $\text{CH}_3\text{NH}_3^+$  site.<sup>14</sup> On the other hand,  $\text{H}^+$  is expected to migrate towards the adjacent iodide atom forming an I – H complex.<sup>14,15</sup> From first principle calculations it is expected that this complex introduces a localized state at  $E_c - E = 50$  meV.<sup>14</sup> It is conceivable that the observed defect luminescence at 1.51 eV is due to I – H complexes that are generated during the exposure to light with a photon energy of  $E_{ph} = 3.4$  eV.

Annealing at 30 K causes a reverse reaction. The I – H complexes dissociate and the H atom can migrate back to the methylamine molecule forming a  $\text{CH}_3\text{NH}_3^+$  ion. The threshold of 30 K directly implies a low kinetic barrier for this reaction. However, the initial state is not completely recovered during the low-temperature anneal (see Fig. 1). This might be due to an incomplete dissociation of I – H complexes and hence, a partial reverse reaction or a change of the perovskite properties in the near-surface region. Although the degradation and annealing experiments were performed at very low temperatures it is conceivable that the generated  $\text{CH}_3\text{NH}_2$  molecules and protons close to the surface can leave the specimens. This would result in a partial recovery of the band-to-band PL, while the defect luminescence vanishes completely.

In summary, we have presented degradation and annealing experiments of  $\text{CH}_3\text{NH}_3\text{PbI}_3$  at  $T \leq 30$  K. Prolonged illumination with  $E_{ph} \geq 2.72$  eV causes the generation of localized defects that reside about 100 meV within the band gap. Defect creation is reversible and a short anneal at  $T = 30$  K causes the localized defects to disappear completely. However, the band-to-band PL at 1.61 eV does not recover completely. FT-IR spectra show a loss of N – H complexes due to light exposure indicating the dissociation of  $\text{CH}_3\text{NH}_3^+$  cations into  $\text{CH}_3\text{NH}_2$  and protons/H atoms. This

is consistent with a recent report on light-induced degradation of perovskites at room temperature.<sup>7</sup>

### Acknowledgements

O.S. acknowledges the Graduate School Hybrid4Energy for financial support. V.V.B. acknowledges the Alexander-von-Humboldt Foundation for financial support in the framework of the Georg Forster Research Fellowship.

### References

- <sup>1</sup> P. Löper, M. Stuckelberger, B. Niesen, J. Werner, M. Filipič, S.-J. Moon, J.-H. Yum, M. Topič, S. De Wolf, and C. Ballif, *J. Phys. Chem. Lett.* **6**, 66 (2015).
- <sup>2</sup> S.D. Stranks, G.E. Eperon, G. Grancini, C. Menelaou, M.J.P. Alcocer, T. Leijtens, L.M. Herz, A. Petrozza, and H.J. Snaith, *Science* **342**, 341 (2013).
- <sup>3</sup> T. Dittrich, F. Lang, O. Shargaieva, J. Rappich, N.H. Nickel, E. Unger, and B. Rech, *Appl. Phys. Lett.* **109**, 73901 (2016).
- <sup>4</sup> O. Shargaieva, F. Lang, J. Rappich, T. Dittrich, M. Klaus, M. Meixner, C. Genzel, and N.H. Nickel, *ACS Appl. Mater. Interfaces* **9**, 38428 (2017).
- <sup>5</sup> W.S. Yang, B.-W. Park, E.H. Jung, N.J. Jeon, Y.C. Kim, D.U. Lee, S.S. Shin, J. Seo, E.K. Kim, J.H. Noh, and S. Il Seok, *Science* **356**, 1376 (2017).
- <sup>6</sup> F. Lang, O. Shargaieva, V. V. Brus, H.C. Neitzert, J. Rappich, and N.H. Nickel, *Adv. Mater.* 1702905 (2017).
- <sup>7</sup> N.H. Nickel, F. Lang, V. V. Brus, O. Shargaieva, and J. Rappich, *Adv. Electron. Mater.* **3**, 1700158 (2017).
- <sup>8</sup> N.J. Jeon, J.H. Noh, Y.C. Kim, W.S. Yang, S. Ryu, and S. Il Seok, *Nat. Mater.* **13**, 897 (2014).
- <sup>9</sup> F. Lang, N.H. Nickel, J. Bundesmann, S. Seidel, A. Denker, S. Albrecht, V. V. Brus, J. Rappich, B. Rech, G. Landi, and H.C. Neitzert, *Adv. Mater.* **28**, 8726 (2016).
- <sup>10</sup> R.L. Milot, G.E. Eperon, H.J. Snaith, M.B. Johnston, and L.M. Herz, *Adv. Funct. Mater.* **25**, 6218 (2015).
- <sup>11</sup> S.M. Sze, *Physics of Semiconductor Devices*, 2nd ed. (John Wiley & Sons, Inc, New York, 1981).
- <sup>12</sup> T. Dittrich, *Materials Concepts for Solar Cells*, 1st ed. (Imperial College Press, London, 2014).
- <sup>13</sup> J.M. Azpiroz, E. Mosconi, J. Bisquert, and F. De Angelis, *Energy Environ. Sci.* **8**, 2118 (2015).
- <sup>14</sup> P. Delugas, A. Filippetti, and A. Mattoni, *Phys. Rev. B* **92**, 45301 (2015).
- <sup>15</sup> D.A. Egger, L. Kronik, and A.M. Rappe, *Angew. Chemie Int. Ed.* **54**, 12437 (2015).

